

Vibrational Analysis of Single Molecule Chemistry: Ethylene Dehydrogenation on Ni(110)

J. Gaudioso, H. J. Lee, and W. Ho*

Contribution from the Laboratory of Atomic and Solid State Physics and Cornell Center for Materials Research, Cornell University, Ithaca, New York 14853

Received April 16, 1999

Abstract: The dynamics and chemistry of individual ethylene molecules adsorbed on the Ni(110) surface at 13 K have been studied with a variable temperature scanning tunneling microscope (STM). By applying a voltage pulse to a single ethylene molecule, the tunneling electrons cause the molecule to reversibly hop away from and back under the tip. The five ethylene isotopes hop at different rates. A larger voltage pulse (1.1–1.5 V) induces dehydrogenation, and a strong primary isotope effect is observed. By using inelastic electron tunneling spectroscopy (IETS) with the STM, we identified the dehydrogenated products from the characteristic vibrational energies as acetylene. This identification is further supported with STM-IETS on single acetylene molecules adsorbed directly from the gas phase. Two different types of acetylene exist on the surface. They can be distinguished in the regular STM image, and they exhibit shifted vibrational peaks. Applying another voltage pulse (1.0–4.8 V) further dehydrogenates acetylene to carbon atoms.

Introduction

The desire to achieve control of chemistry ultimately requires an understanding of reactions at the single molecule level. The unique capabilities of the scanning tunneling microscope (STM) enable one to manipulate^{1–3}, excite^{4–7}, and dissociate^{8–11} single molecules, effectively leading to a reactor of molecular dimensions. Until recently, the STM lacked chemical sensitivity, making it difficult to identify the reactants and products. Inelastic electron tunneling spectroscopy (IETS) with the STM¹² opens the possibility of using the characteristic vibrational frequencies to identify single molecules.

By using the STM for excitation and as a probe, we have been able to manipulate and study ethylene and acetylene adsorbed on Ni(110). A voltage pulse applied between the tip and sample can reversibly hop ethylene molecules away from and back under the tip. Applying a larger voltage pulse transforms a single ethylene molecule into an acetylene. STM-IETS can identify the product of this single molecule reaction. This chemical identification is particularly important because there are several plausible products. Thermally, ethylene can

decompose to ethylidyne (CH₃C) on Pt(111),¹³ acetylene on Ni(111),¹⁴ vinyl (CHCH₂) on Pd(100)¹⁵ and on Ni(100),^{16,17} and ethynyl (CCH) on Ni(110)¹⁸ and on Pd(110).¹⁹

There has been widespread interest in the chemisorption and decomposition of ethylene and acetylene on single crystal transition metal surfaces because these systems serve as models for catalytic hydrogenation and dehydrogenation reactions. Most of these investigations have been carried out with macroscopic techniques such as high resolution electron energy loss spectroscopy (HREELS),^{16–20} temperature programmed desorption (TPD),^{16–19,21} ultraviolet (UV) photoemission spectroscopy (UPS),¹⁴ static secondary ion mass spectrometry (SSIMS),^{22,23} and near edge X-ray absorption fine structure spectroscopy (NEXAFS).^{13,24} The STM, in contrast, reveals information about the local environment of the molecules to be studied. The adsorption sites of ethylene on Cu(110)²⁵ and on Pd(110)²⁶ and of acetylene on Pd(111)²⁷ and on Cu(100)¹² have been successfully determined via STM studies. The STM has also been used

- (1) Eigler, D. M.; Schweizer, E. K. *Nature* **1990**, *344*, 524–526.
- (2) Crommie, M. F.; Lutz, C. P.; Eigler, D. M. *Science* **1993**, *262*, 218–220.
- (3) Gimzewski, J. K.; Joachim, C. *Science* **1999**, *283*, 1683–1688.
- (4) Eigler, D. M.; Lutz, C. P.; Rudge, W. E. *Nature* **1991**, *352*, 600–603.
- (5) Stipe, B. C.; Rezaei, M. A.; Ho, W. *Science* **1998**, *279*, 1907–1909.
- (6) Stipe, B. C.; Rezaei, M. A.; Ho, W. *Phys. Rev. Lett.* **1998**, *81*, 1263–1266.
- (7) Swartzentruber, B. S.; Smith, A. P.; Jónsson, H. *Phys. Rev. Lett.* **1996**, *77*, 2518–2521.
- (8) Dujardin, G.; Walkup, R. E.; Avouris, Ph. *Science* **1992**, *255*, 1232–1235.
- (9) Shen, T. C.; Wang, C.; Abeln, G. C.; Tucker, J. R.; Lyding, J. W.; Avouris, Ph.; Walkup, R. E. *Science* **1995**, *268*, 1590–1592.
- (10) Stipe, B. C.; Rezaei, M. A.; Ho, W.; Gao, S.; Persson, M.; Lundqvist, B. I. *Phys. Rev. Lett.* **1997**, *78*, 4410–4413.
- (11) Rezaei, M. A.; Stipe, B. C.; Ho, W. *J. Chem. Phys.* **1998**, *109*, 6075–6078.
- (12) Stipe, B. C.; Rezaei, M. A.; Ho, W. *Science* **1998**, *280*, 1732–1735.

- (13) Gland, J. L.; Zaera, F.; Fischer, D. A.; Carr, R. G.; Kollin, E. B. *Chem. Phys. Lett.* **1988**, *151*, 227–229.
- (14) Demuth, J. E. *Surf. Sci.* **1978**, *76*, L603–L608.
- (15) Stuve, E. M.; Madix, R. J. *J. Phys. Chem.* **1985**, *89*, 105–112.
- (16) Zaera, F.; Hall, R. B. *Surf. Sci.* **1987**, *180*, 1–18.
- (17) Zaera, F.; Hall, R. B. *J. Phys. Chem.* **1987**, *91*, 4318–4323.
- (18) Stroschio, J. A.; Bare, S. R.; Ho, W. *Surf. Sci.* **1984**, *148*, 499–525.
- (19) Nishijima, M.; Yoshinobu, J.; Sekitani, T.; Onchi, M. *J. Chem. Phys.* **1989**, *90*, 5114–5127.
- (20) Bandy, B. J.; Chesters, M. A.; Pemble, M. E.; McDougall, G. S.; Sheppard, N. *Surf. Sci.* **1984**, *139*, 87–97.
- (21) Weinelt, M.; Huber, W.; Zebisch, P.; Steinrück, H. P.; Pabst, M.; Rösch, N. *Surf. Sci.* **1992**, *271*, 539–554.
- (22) Zhu, X. Y.; Castro, M. E.; Akhter, S.; White, J. M.; Houston, J. E. *Surf. Sci.* **1988**, *207*, 1–16.
- (23) Tjandra, S.; Zaera, F. *Langmuir* **1991**, *7*, 1432–1435.
- (24) Weinelt, M.; Huber, W.; Zebisch, P.; Steinrück, H. P.; Ulbricht, P.; Birkenheuer, U.; Boettger, J. C.; Rösch, N. *J. Chem. Phys.* **1995**, *102*, 9707–9724.
- (25) Doering, M.; Buisset, J.; Rust, H. P.; Briner, B. G.; Bradshaw, A. M. *Faraday Discuss.* **1996**, *105*, 163–175.
- (26) Ichihara, S.; Yoshinobu, J.; Ogasawara, H.; Nantoh, M.; Kawai, M.; Domen, K. *J. Electron Spectrosc. Relat. Phenom.* **1998**, *88–91*, 1003–1007.

to follow the thermal decomposition of ethylene \rightarrow ethylidyne \rightarrow carbon particles \rightarrow graphite on Pt(111).²⁸

Experimental Section

All experiments were conducted with a homemade, variable-temperature STM²⁹ operating in ultrahigh vacuum (2×10^{-11} Torr base pressure). The Ni(110) sample was cleaned by repeated Ne ion sputtering and annealing to 725 °C. Oxidation and reduction cycles with O₂ and H₂, respectively, further reduced the carbon contamination. Etched polycrystalline tungsten tips were also sputtered and annealed prior to use. For experiments, the sample and microscope were cooled to 13 K. Then the surface was dosed in-situ with the molecules of interest. The various isotopes of ethylene and acetylene were dosed in sequence. Scanning the surface between dosing the different species enabled us to monitor coverage and map out the locations of the molecules. To ensure a sufficient number of isolated molecules, we dosed no more than seven species during a given experiment and the total coverage was less than 0.003 monolayer.

STM topographical images were taken with a tunneling current of 1 nA and a sample bias of 250 mV. Under these conditions, ethylene appears as a protrusion and acetylene appears as a depression in the constant current images. To induce hopping of the ethylene molecules, the tip was placed over the maximum height of a molecule, the feedback was turned off, and a 10 s voltage pulse of 1 V was applied. During this pulse, the tip remained stationary as the molecule hopped away from and back under the tip. To dehydrogenate the ethylene and acetylene, we again placed the tip over a maximum for ethylene or a minimum for acetylene. With the feedback off, a 10 s voltage pulse was applied. Voltage pulses of 1.00–1.80 V, in increments of 50 mV, were used for ethylene. Acetylene dehydrogenation required voltage pulses in the range of 1.00–4.80 V.

To obtain a vibrational spectrum,^{12,29} we tracked the molecule on a local minimum or maximum in the topographical image. The feedback was then turned off; an ac modulation (7 mV, 200 Hz) was added to the linearly ramped dc sample bias voltage. A lock-in amplifier was used to detect the first and second harmonics of the modulation frequency which are proportional to dI/dV and d^2I/dV^2 , respectively. After each sweep of the bias voltage, the feedback was turned back on and the molecule was tracked automatically prior to the next sweep. Spectra were averaged after each sweep. One pass from 200 to 400 mV and back to 200 mV takes about 1 min. The vibrational energies are reported in units of millielectronvolts: 1 meV = 8.0655 cm^{-1} .

Results

Previous investigations of ethylene and acetylene adsorbed on Ni(110)^{18,20,21,24,30} have provided some information on binding sites. Indirect evidence from HREELS¹⁸, angle-resolved UV photoemission spectroscopy (ARUPS)²¹, and angle-resolved inverse photoemission spectroscopy (ARIPS)³⁰ points to ethylene adsorbing on top of the Ni(110) rows. Similarly, experiments by HREELS,^{18,20} ARUPS,²⁴ and NEXAFS²⁴ imply that acetylene adsorbs in the Ni(110) troughs. As can be seen in Figure 1, our STM results provide direct confirmation for both of these assignments. Although the individual atoms are not resolved, the Ni(110) rows are distinct. It is evident in these STM images that ethylene adsorbs on top of the rows and acetylene adsorbs over the troughs.

To our knowledge, these are the first STM images of acetylene on Ni(110). As expected, the constant current images of acetylene isotopes (C₂H₂, C₂HD, and C₂D₂) appear the same.

(27) Dunphy, J. C.; Rose, M.; Behler, S.; Ogletree, D. F.; Salmeron, M.; Sautet, P. *Phys. Rev. B* **1998**, *57*, R12705–R12708.

(28) Land, T. A.; Michely, T.; Behm, R. J.; Hemminger, J. C.; Comsa, G. *J. Chem. Phys.* **1992**, *97*, 6774–6783.

(29) A variation of the STM described in: Stipe, B. C.; Rezaei, M. A.; Ho, W. *Rev. Sci. Instrum.* **1999**, *70*, 137–143.

(30) Gutdeutsch, U.; Birkenheuer, U.; Bertel, E.; Cramer, J.; Boettger, J. C.; Röscher, N. *Surf. Sci.* **1996**, *345*, 331–346.

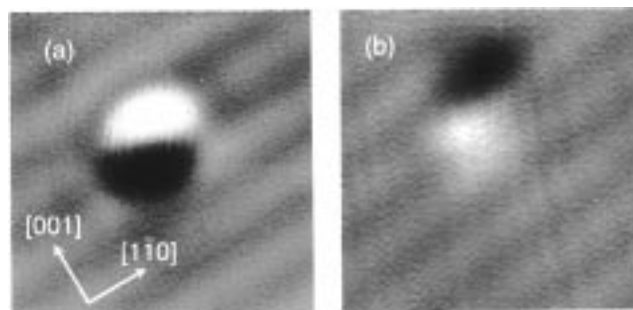


Figure 1. Both images are illuminated from the top in the image processing. (a) STM image of ethylene adsorbed on Ni(110) at 13 K. The protrusion (bright) is located directly on top of the Ni(110) row; this feature is the ethylene molecule. (b) STM image of acetylene adsorbed on Ni(110) at 13 K. The depression (dark) is located directly over a trough. The bright feature is the acetylene anti-shadow (an artifact arising from the illumination).

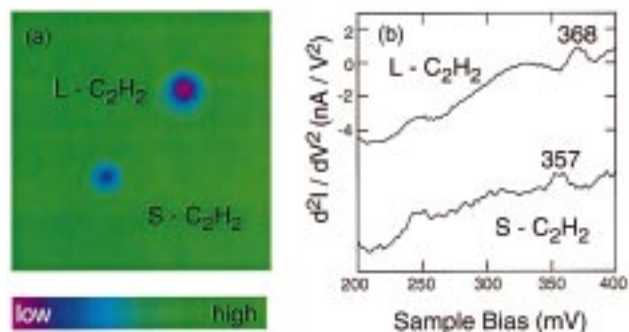


Figure 2. (a) STM image of S-acetylene (small) and L-acetylene (large). (b) The corresponding vibrational spectra for C₂H₂, obtained with the same tip, are shown. The data in panel b are the average of 255 passes for L-C₂H₂ and 40 passes for S-C₂H₂; total data collection times were approximately 510 and 80 min, respectively. The same dwell time per channel is used for all other spectra in the paper; adjacent channels are 2.5 meV apart. The spectra share the same scale for the y-axis but are displaced for clarity.

Acetylene dosed directly on the surface can be of two types (S- and L-). S- and L- refer to the size of the acetylene in the constant current image. In Figure 2a, the L-C₂H₂ image is larger by 1.5 Å in diameter and is 0.17 Å deeper than that of S-C₂H₂. The two acetylene molecules in Figure 2a are separated by 16.7 Å (6.7 lattice spacings) along the trough. Dosing at 13 K produced 37% S-acetylene and 62% L-acetylene. Because acetylene interacts strongly with the surface, STM-induced hopping or interconversion of S-acetylene and L-acetylene was not observed.

STM-IETS can be used to characterize the adsorbed acetylene. The C–H vibrational peak of S-C₂H₂ is red-shifted from that of L-C₂H₂ (Figure 2b). S-Acetylene exhibits a characteristic C–H (C–D) stretch at 357 mV (267 mV), while the C–H (C–D) stretch for L-acetylene is at 368 mV (275 mV). These values differ slightly from the values obtained by HREELS:¹⁸ 374 mV for the C–H stretch in C₂H₂ on Ni(110) and 269 mV for the C–D stretch in C₂D₂ on Ni(110). The d^2I/dV^2 spectra taken with the same tip over the three S-acetylene isotopes, S-C₂H₂, S-C₂HD, and S-C₂D₂, are shown in Figure 3. The relative change in the conductance is defined as $\Delta\sigma/\sigma$ where $\sigma = dI/dV$. This change in ac tunneling conductance for the C–H (C–D) mode in S-C₂HD is approximately half of the observed change for the C–H (C–D) mode in C₂H₂ (C₂D₂). Other vibrational modes of the adsorbed acetylene were not observed. The other features in the spectra do not show isotopic shifts and are attributed to the electronic structure of the tip and

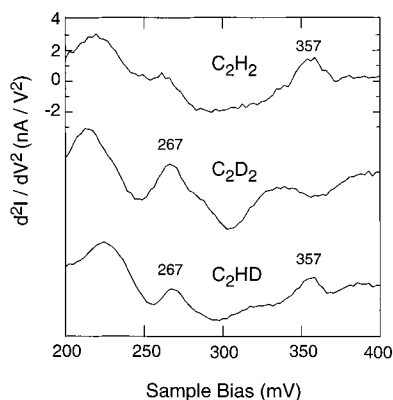


Figure 3. Vibrational spectra for all three S-acetylene isotopes, recorded with the same tip. The spectra are the average of 75, 387, and 31 passes for C₂H₂, C₂D₂, and C₂HD, respectively.

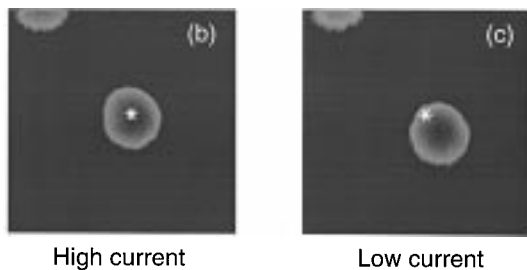
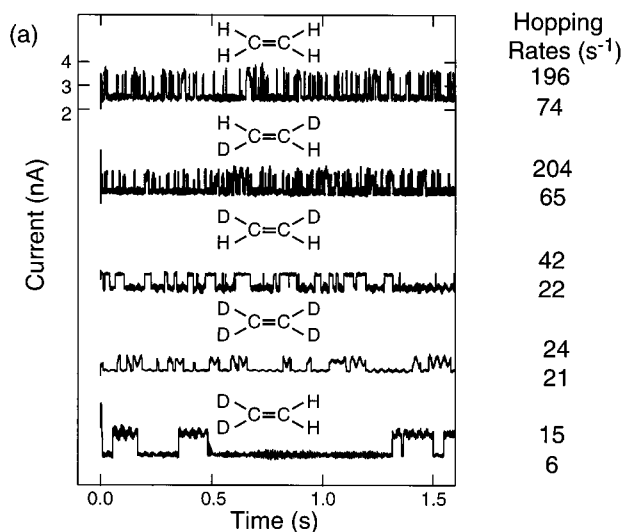


Figure 4. (a) Tunneling current during a 1 V pulse is shown for each ethylene isomer. Next to the high (low) current level for each is the rate at which the molecule hops out from (back under) the tip. (b) STM image of an ethylene under the tip (high current state). The tip position is shown with the asterisk. (c) STM image of ethylene after it has hopped (low current state). The tip remains stationary during hopping.

surface. These features are tip-dependent as can be seen by comparing the spectra in Figures 2, 3, and 9.

The ethylene molecules could not be easily characterized by STM-IETS because they hop under the influence of tunneling electrons. No vibrational peaks were observed for the isotope with the lowest hopping rate (1,1-C₂H₂D₂), even though the molecule remained stationary during the ramping of the sample bias up to 300 mV to probe the C–D stretch. The ethylene isotopes could instead be characterized by their distinct hopping rates (Figure 4a). After imaging an isolated molecule, the tip was positioned over the brightest point in the molecule (a local maximum in the topographical image). The sample bias voltage was then increased to induce hopping, and the time-dependent

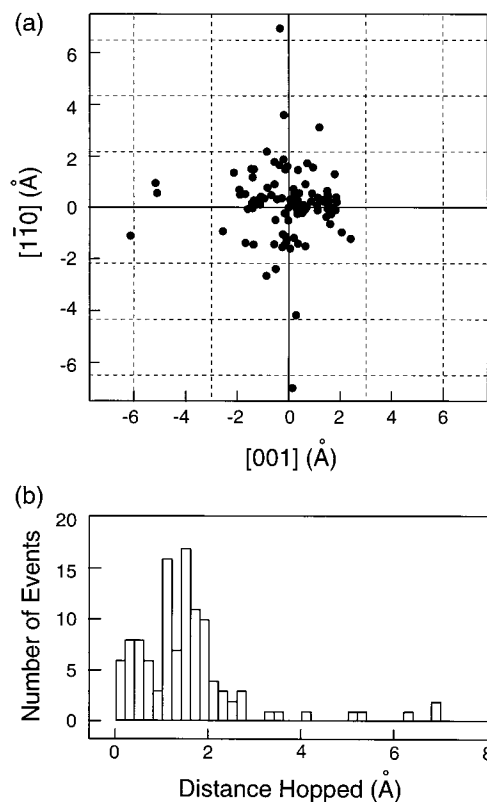


Figure 5. Distribution of hopping of individual ethylene molecules (all isotopes). (a) Each marker (●) represents the distance and direction of hopping for an ethylene molecule. A total of 112 events were analyzed. An isotope effect was not resolved. The dashed grid represents the Ni(110) lattice. (b) The histogram shows the distribution of hopping distance with a bin width of 0.2 Å and a peak at 1.4 Å.

tunneling current was recorded. A drop in the tunneling current indicates that the molecule has moved away from the tip. When the molecule moves back, the tunneling current jumps back up to its original value. During a 10 s voltage pulse, the ethylene molecule can hop away from and back under the tip many times. A rescan of the same area at the end of the voltage pulse shows that the molecule has moved (Figure 4b,c).

A histogram of the time intervals spent in each current state for the hopping of individual ethylene molecules shows an exponential dependence. The hopping rate for a given sample bias voltage and tunneling current is simply the inverse of the time constant of the decay of this exponential. A comparison of the hopping rates between the five ethylene isotopes under the same initial conditions (voltage and current) is shown in Figure 4a. The rate is obtained from analysis of 277–1302 hopping events collected on a total of 8–16 different molecules for each isotope. The same hopping rates were obtained with different tips. However, the difference in the magnitude between the high and low current states is tip-dependent.

The distance and direction of hopping of individual ethylene molecules at the end of the voltage pulse are shown in Figure 5a. No distinct differences in the results are observed for the different isotopes. The origin represents the stationary tip location. The dashed grid corresponds to the lattice spacings (2.49 Å in [110] and 3.45 Å in [001]). There is no clear preference for movement along a particular crystallographic axis. The distribution of distance hopped is plotted in Figure 5b. These results may be related to the observation that the constant current image of an ethylene molecule directly after dosing at 13 K is different than the image of an ethylene molecule once it

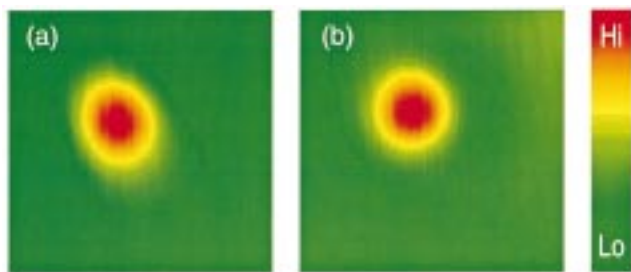


Figure 6. *cis*-C₂H₂D₂ (a) before hopping (directly after dosing) (b) after hopping. The molecule continued to image as in part b regardless of whether it had been hopped once or many times. All isotopes showed this distinction with a sharp tip.

Table 1. Threshold Voltages for STM-Induced Dehydrogenation of Ethylene to Acetylene and Acetylene to Carbon^a

ethylene	C ₂ H ₄	1.14 ± 0.07	S-acetylene	C ₂ H ₂	1.35 ± 0.11
	<i>cis</i> -C ₂ H ₂ D ₂	1.23 ± 0.09		C ₂ D ₂	2.18 ± 0.81
	1,1-C ₂ H ₂ D ₂	1.37 ± 0.09	L-acetylene	C ₂ H ₂	1.14 ± 0.07
	<i>trans</i> -C ₂ H ₂ D ₂	1.46 ± 0.11		C ₂ D ₂	4.52 ± 0.45
	C ₂ D ₄	1.47 ± 0.12			

^a For each isotope, threshold voltages were determined from 30–40 ethylene and 9–15 acetylene molecules.

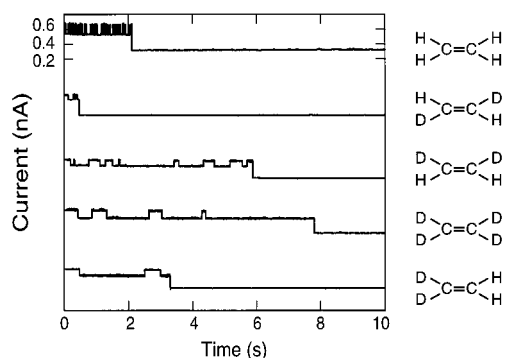


Figure 7. The tunneling current is shown from a 10 s voltage pulse that induces dehydrogenation. The applied sample bias voltages are 1.00, 1.40, 1.20, 1.50, and 1.40 V from top to bottom current traces. Notice that the molecule hops back and forth before dissociating (the final decrease in the current). Ethylene can dissociate from either the high or low current state (under or away from the tip).

has hopped, as shown in Figure 6. For all isotopes studied and with all tips, the image before hopping is distinct from that after hopping.

In addition to inducing motion in the individual ethylene molecules, the STM can also induce dehydrogenation of single ethylene molecules. During a 10 s voltage pulse of the appropriate magnitude (1.1–1.5 V; see Table 1), the molecule would hop until it dissociated. This dehydrogenation was evident by an even larger change in the tunneling current (Figure 7, Figure 8b). Rescanning the same area after this sudden drop in tunneling current produced an image that was significantly different than the initial image of ethylene. Ethylene appeared as a protrusion in the topographical image (Figure 8a), while this product appeared as a depression (Figure 8c).

STM-IETS was used to identify this product. The vibrational spectrum of the product exhibits a peak with its position, width, and intensity just like the C–H stretch in adsorbed C₂H₂. Likewise, the vibrational spectrum of a dehydrogenated C₂D₄ molecule shows the same C–D peak as deuterated acetylene (C₂D₂). A strong primary isotope effect is observed in the dehydrogenation of the other three isotopes. Only the C–D stretch is observed after STM-induced dehydrogenation of *trans*-

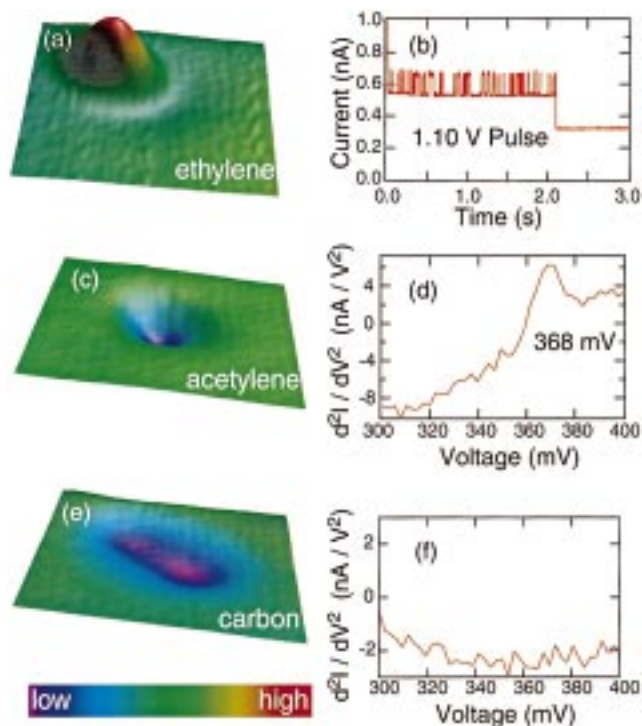


Figure 8. (a) STM image of C₂H₄. The C₂H₄ image has a height of 0.75 Å above the surface. (b) Pulse (1.1 V) of 10 s duration (only the first 3 s are shown) applied with the tip over the maximum of the C₂H₄ image. The sharp decrease in current after 2 s signals the dehydrogenation of ethylene. (c) STM image taken after the 10 s pulse in part b. The C₂H₂ images as a depression of −0.54 Å. (d) d^2I/dV^2 recorded directly over the center of the molecular image in part c, showing a C–H peak at 368 mV. This spectrum is an average of 50 passes. (e) STM image after applying a 2 V pulse over the molecule imaged in part c. The carbon atoms image as depressions 0.22 Å deep and 5.0 Å apart. (f) d^2I/dV^2 taken over the center of the image in part e; the C–H peak is no longer present.

C₂H₂D₂, *cis*-C₂H₂D₂, and 1,1-C₂H₂D₂, implying a remarkable isotope selectivity for adsorbed molecules.

Figure 9 shows the vibrational spectra for all of the dehydrogenated ethylene species. A small secondary isotope effect is observed in the dissociation of the three C₂H₂D₂ isotopes. These three isotopes fall between C₂H₄ and C₂D₄ in the ease of dehydrogenation, with *cis*-C₂H₂D₂, the easiest of the three, followed by 1,1-C₂H₂D₂, and *trans*-C₂H₂D₂. The ease of dehydrogenation was determined from the threshold voltage at which the reaction was observed. The tip was placed over an isolated molecule, and a low voltage pulse of 10 s duration was applied. If dehydrogenation, as indicated by a sharp current drop, did not occur, the tip was repositioned over the molecule and the voltage increased by 50 mV. The tip height was adjusted to keep the tunneling current approximately constant. Dehydrogenation was carried out for 30–40 molecules of each isotope to determine an average threshold voltage.

One of the thermal decomposition products of ethylene on Ni(110) was attributed to a CCH species.¹⁸ To eliminate this as a possible STM-induced product and to further confirm our identification, we adsorbed acetylene molecules directly on the surface. The same tip was used to record the vibrational spectra, shown in Figure 9, for acetylene, deuterated acetylene, and the STM-induced dehydrogenated ethylene products. While the position of a vibrational peak remains the same, its intensity and line shape depend on the tip conditions. Therefore, changes in the tip (e.g. rearrangement of the atoms or the adsorption of impurities on the tip) would invalidate quantitative comparisons

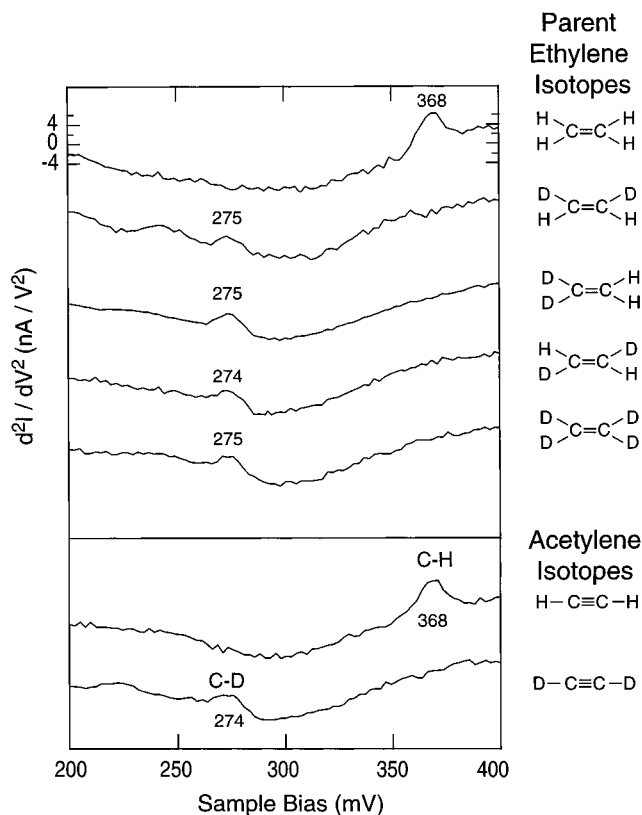


Figure 9. Vibrational spectra taken of C_2H_2 , C_2D_2 , and the products of STM-induced dehydrogenation of the five ethylene isotopes. The energies of the peaks reveal that these acetylene products are L-type. The spectrum of dehydrogenated 1,1- $C_2H_2D_2$ is the average of 368 passes, demonstrating the improvement in the signal-to-noise ratio. Each of the other spectra is the average of 50 passes. All spectra were recorded with the same tip and share the same scale for the y-axis.

between spectra for different molecules on the surface. If the same tip is used, comparison of the vibrational peaks is reliable even if we do not yet have a rigorous understanding of the origin of the observed intensities. Thus, all spectra within a given figure have been obtained with the same tip. Tips which produce the sharpest topographical images generally give higher intensity peaks. The typical range observed for the relative change in ac conductance ($\Delta\sigma/\sigma$) was 0.5–6% for the C–H and C–D stretch of acetylene on Ni(110). The magnitude of the relative change in the ac conductance depends on both the tip and the isotope.

The spectra of C_2H_2 and C_2D_2 are also shown in Figure 9 for comparison with the dehydrogenated ethylene products. It is evident that the C–H (C–D) stretch in dehydrogenated C_2H_4 (C_2D_4 , trans- $C_2H_2D_2$, cis- $C_2H_2D_2$, and 1,1- $C_2H_2D_2$) has the same frequency and intensity and a similar line shape as that for the C–H stretch in C_2H_2 (C_2D_2). The quantitative agreement in these spectra means that there are two C–H (C–D) bonds in the STM-induced product. In contrast, the proposed CCH product in the thermal decomposition contains only one C–H bond. If there was only one C–H bond present, we would expect a C–H vibrational peak with approximately half the intensity, as is seen in the vibrational spectrum of C_2HD compared to that of C_2H_2 (Figure 3b). Therefore, by using single molecule STM-IETS, one can identify the product of the STM-induced dehydrogenation of ethylene as acetylene.

Dehydrogenation of the ethylene isotopes could produce either type of acetylene; however L-acetylene was favored. For those products, which were identified with IETS, 80% were L-acetylene regardless of which ethylene isotope was the reactant.

Each type of acetylene could undergo further STM-induced dehydrogenation. Figure 8e shows a three-dimensional topographical STM image of dissociated acetylene, revealing two depressions. The spectra for these products showed no peaks that could be associated with C–H or C–D vibrations (Figure 8f). These results lead to the conclusion that STM-induced dehydrogenation of an acetylene molecule on Ni(110) removes both remaining hydrogen atoms, leaving just two carbon atoms. Again, there is a strong primary isotope effect; C_2H_2 dehydrogenates significantly easier than C_2D_2 . The two different types of acetylene dehydrogenate at distinct voltages. For C_2H_2 , the L-type dehydrogenates at a lower voltage than the S-type. However, for C_2D_2 , the order is reversed, with the S-type dehydrogenating at a lower voltage than the L-type. A summary of the threshold voltage for the dehydrogenation of ethylene and acetylene isotopes is given in Table 1.

Discussion

A thorough study of the vibrational spectra of acetylene on various transition metals has led to two proposed structures.³¹ In one structure, acetylene can σ -bond to two metal atoms and π -bond to a third. In the other structure, the acetylene bonds to four metal atoms through two σ -bonds and two π -bonds. Previous studies classified acetylene adsorbed on Ni(110) at 120 and 80 K as having the first structure.³¹

There is very little evidence in the literature for two types of acetylene coexisting on the same surface. In a HREELS study of acetylene on Ni(110) at 80 K,¹⁸ a broad C–H stretch was observed and deconvoluted into two peaks separated by 14.3 meV. This peak splitting was attributed to the two CH groups in C_2H_2 being in different environments. Alternatively, the two peaks could be a result of two types of coexisting acetylene. The two types of acetylene observed by STM on Ni(110) are most likely bound in two different adsorption sites. Although both S-acetylene and L-acetylene are bound over the trough, they are separated by a nonintegral number of lattice spacings, implying the occupation of different sites. This is further supported by the 11 mV shift in the vibrational peaks between L-acetylene and S-acetylene.

If the C–H stretch energies of adsorbed S- C_2H_2 and L- C_2H_2 are compared to those of gaseous C_2H_2 (sp), C_2H_4 (sp^2), and C_2H_6 (sp^3),³² it is evident that the carbon in S- C_2H_2 has mostly sp^3 character and that in L- C_2H_2 has more sp^2 character. These different carbon hybridizations correspond to different molecule–surface interactions and thus different adsorption geometries for the two observed types of acetylene. Recently, direct evidence for two types of coexisting acetylene²⁷ has been found on Pd(111). Acetylene was observed with the STM to occupy two different 3-fold hollow binding sites on Pd(111) below 70 K. Only one type of adsorbed acetylene was found in other low-temperature STM studies of acetylene on Cu(110),³³ Cu(100),³⁴ and Ni(100).³⁴

Although no vibrational peaks were observed for ethylene by STM-IETS, the tunneling electrons can be used to manipulate single adsorbed ethylene molecules. Hopping a molecule away from and back under the stationary tip requires energy transfer from the tunneling electrons to the molecule. A similar

(31) Sheppard, N. *Annu. Rev. Phys. Chem.* **1988**, *39*, 589–644.

(32) Herzberg, G. *Molecular Spectra and Molecular Structure, II. Infrared and Raman Spectra of Polyatomic Molecules*; Krieger Publishing Co.: Malabar, FL, 1991; pp 288–293 and 325–328.

(33) Lauhon, L.; Ho, W. Adsorption studies of acetylene on Cu(110), 1998, unpublished results.

(34) Stipe, B. C.; Rezaei, M. A.; Ho, W. *Phys. Rev. Lett.* **1999**, *82*, 1724–1727.

mechanism is also responsible for the tunneling electron-induced displacement of Si atoms on Si(111)-(7 × 7).³⁵ In contrast, STM manipulation of surface adsorbates has been achieved through either a repulsive (pushing) or attractive (pulling) mechanism where the tip is placed closer to the surface.^{1,2,36–38}

The ethylene isotopes hop at distinct rates (Figure 4a). With the exception of the C₂H₄ and trans-C₂H₂D₂ species, the hopping rates for the other three isotopes are visually distinguishable by observing the tunneling current during the voltage pulse. This provides a quick confirmation of the identity of the isotope selected for dehydrogenation. A few other isotope studies with an STM have been undertaken. An isotope-dependent rate was observed for the STM-induced rotation of acetylene on Cu(100)⁶ and the hopping of a CO molecule from Cu(111) to the tip.³⁹

The five isotopes of ethylene can be divided into two groups. C₂H₄ hops significantly faster than C₂D₄. This could be attributed to the difference in mass between these two isotopes. The other three C₂H₂D₂ isotopes, identical in mass, have sizable differences in hopping rate. The trans-C₂H₂D₂ hops faster than cis-C₂H₂D₂, which hops faster than 1,1-C₂H₂D₂. This ordering parallels a change in the center of mass for these isotopes. For trans-C₂H₂D₂, the center of mass is in the center of the molecule; for 1,1-C₂H₂D₂ the center of mass is the furthest from the molecule's geometric center. This is a plausible explanation of the observation; other explanations are possible, but we do not have direct evidence for them.

Another contributing factor in the observed rates could be the variations in the zero point vibrational energy for the isotopes. For a molecule to move across the surface, hopping to the next site, it must acquire enough energy to surmount the barrier to diffusion. Two vibrational modes, the surface-molecule and hindered translation vibrations, are important components of this reaction coordinate. The importance of these modes for diffusion has been observed in He scattering experiments for CO adsorbed on Cu(001).⁴⁰ The ethylene isotopes have different zero-point vibrational energies for these motions, and isotope-dependent diffusion rates have been seen for hydrogen versus deuterium on Ni(001).⁴¹ With the STM-induced motion, the tunneling electrons inelastically scatter from an adsorbed molecule, transferring energy to the vibrational modes of the molecule.⁴² One or more excitations in a vibrational ladder climbing process can provide enough energy to overcome the barrier to motion.

From Figure 5a, it is clear that the ethylene hopping distances are nonintegral in the lattice spacings, suggesting that the molecule experiences a relatively homogeneous interaction potential with the surface. Once the molecule has been hopped initially, a return to its original state (as determined from the STM images) was not observed. The difference in the constant current images of ethylene taken before and after hopping (Figure 6a,b) may indicate a correlation between this change

and the interaction potential. Constant current images are related to the spatial distribution of the local density of states. Therefore, a change in the image indicates a change in the electronic structure of the ethylene. STM images have been shown to be sensitive to molecule-surface interactions. Calculations for CO⁴³ and benzene⁴⁴ on Pt(111) show a site dependence of the contrast in the STM images that agrees well with experiment.

Inelastic scattering of tunneling electrons can transfer sufficient energy to break molecular bonds. This was shown to be the mechanism for the STM-induced dissociation of single O₂ molecules adsorbed on Pt(111).¹⁰ Inelastic scattering can also cause the degradation of larger molecules. Scanning regions of the Si(111)-(7 × 7) surface with the sample biased at ≥4 V induces the dissociation of adsorbed B₁₀H₁₄ molecules.⁸ Energetic electrons can be used to remove a lobe from the four-lobed Cu-tetra-3,5 di-tertiary-butyl-phenyl porphyrin molecule.⁴⁵

Inelastic scattering of tunneling electrons from ethylene provides a mechanism for inducing dehydrogenation. A possible mechanism for the observed strong primary isotope effect lies in the differences in the zero point energies between C-H and C-D vibrations. Because the C-H bond is always the first one to dissociate in the three C₂H₂D₂ isotopes, producing exclusively C₂D₂, the effects of the zero point energy differences in the gas phase must be accentuated for the adsorbed molecules. In the dehydrogenation of gaseous C₂H₂D₂ isomers, C₂H₂, C₂HD, and C₂D₂ products are observed.^{46,47} In contrast, a substantial primary isotope effect is observed for adsorbed ethylene.^{13,16,17,22} A SSIMS study²³ of the decomposition of C₂D₃H to a vinyl moiety (C₂D₃) shows exclusive breaking of the C-H bond.

Another mechanism to explain the isotope effect observed in dehydrogenation is based on the Menzel-Gomer-Redhead (MGR) model^{48,49} for electron stimulated desorption (ESD). The MGR model has been used to successfully explain isotope effects observed for desorption probabilities in ESD studies.^{50–53} For ESD of H⁺ and D⁺ ions from W(100), the H⁺ ion yield is more than 100 times greater than the D⁺ ion yield.⁵¹

An adsorbed molecule can be excited by the tunneling electrons via a Franck-Condon transition to a higher electronic state. For dehydrogenation reactions, the reaction coordinate involves the C-H and C-D bonds. While in the excited state, the H and the D in these bonds gain kinetic energy. Upon relaxation via another Franck-Condon transition, a gain in the potential energy is obtained since the bonds are no longer at their equilibrium distances. While the electronic structure, the excited-state lifetime, and the bond strength are independent of the isotope, the total energy gained in the excitation-relaxation cycle for the C-H bond is greater than that of the C-D bond and is predominately kinetic in nature.⁵⁴ In cases where bond dissociation occurs directly from the excited state, for example, from a repulsive potential curve, the greater velocity of the H

(43) Bocquet, M. L.; Sautet, P. *Surf. Sci.* **1996**, *360*, 128–136.

(44) Sautet, P.; Bocquet, M. L. *Surf. Sci.* **1994**, *304*, L445–L450.

(45) Gimzewski, J. K.; Jung, T. A.; Cuberes, M. T.; Schlittler, R. R. *Surf. Sci.* **1997**, *386*, 101–114.

(46) Chang, A. H. H.; Mebel, A. M.; Yang, X. M.; Lin, S. H.; Lee, Y. T. *J. Chem. Phys.* **1998**, *109*, 2748–2761.

(47) Lin, J. J.; Hwang, D. W.; Lee, Y. T.; Yang, X. *J. Chem. Phys.* **1998**, *109*, 2979–2982.

(48) Menzel, D.; Gomer, R. *J. Chem. Phys.* **1964**, *41*, 3311–3328.

(49) Redhead, P. A. *Can. J. Phys.* **1964**, *42*, 886–905.

(50) Madey, T. E.; Yates, J. T.; King, D. A.; Uhlaner, C. J. *J. Chem. Phys.* **1970**, *52*, 5215–5220.

(51) Madey, T. E. *Surf. Sci.* **1973**, *36*, 281–294.

(52) Leung, C.; Steinbrüchel, C.; Gomer, R. *Appl. Phys.* **1977**, *14*, 79–87.

(53) Ramsier, R. D.; Yates, J. T. *Surf. Sci. Rep.* **1991**, *12*, 243–378.

(54) Zimmermann, F. M.; Ho, W. *J. Chem. Phys.* **1994**, *100*, 7700–7706.

(35) Stipe, B. C.; Rezaei, M. A.; Ho, W. *Phys. Rev. Lett.* **1997**, *79*, 4397–4400.

(36) Bartels, L.; Meyer, G.; Rieder, K. H. *Phys. Rev. Lett.* **1997**, *79*, 697–700.

(37) Jung, T. A.; Schlittler, R. R.; Gimzewski, J. K.; Tang, H.; Joachim, C. *Science* **1996**, *271*, 181–184.

(38) Cuberes, M. T.; Schlittler, R. R.; Gimzewski, J. K. *Appl. Phys. Lett.* **1996**, *69*, 3016–3018.

(39) Bartels, L.; Meyer, G.; Rieder, K. H.; Velic, D.; Knoesel, E.; Hotzel, A.; Wolf, M.; Ertl, G. *Phys. Rev. Lett.* **1998**, *80*, 2004–2007.

(40) Graham, A. P.; Hofmann, F.; Toennies, J. P.; Williams, G. P.; Hirschmugl, C. J.; Ellis, J. *J. Chem. Phys.* **1998**, *108*, 7825–7834.

(41) Mattsson, T. R.; Wahnström, G. *Phys. Rev. B* **1997**, *56*, 14944–14947.

(42) Ho, W. *Acc. Chem. Res.* **1998**, *31*, 567–573.

compared to the D favors the dissociation of the C–H bond, which directly competes with electronic relaxation. In the MGR model, the total energy gained depends on $m^{-1/2}$, where m is the mass of the departing species (H or D).⁵⁴ The greater total energy gained combined with the higher zero point vibrational energies contribute to the isotope selectivity observed for the dehydrogenation of $C_2H_2D_2$ to produce exclusively C_2D_2 .

In addition to inducing the dehydrogenation of ethylene to acetylene, the STM can also yield additional insights into the mechanism of this reaction. The STM images show that one important step in the dehydrogenation is the migration of ethylene from on top of the Ni row to over the trough for acetylene. It is not possible to conclude whether this translation occurs in concert with or after the elimination of hydrogen.

There are two possible pathways for this hydrogen elimination. The hydrogen can detach as H_2 or as 2 H. Molecular elimination would likely be easiest for the 1,1- $C_2H_2D_2$ isomer; the hydrogen atoms are farther apart in cis- $C_2H_2D_2$ and trans- $C_2H_2D_2$ isomers. For the latter two, a likely scenario for H_2 elimination requires rearrangement prior to elimination.

The other possibility involves the loss of two hydrogen atoms. This is apparently the case for the thermal dehydrogenation of adsorbed ethylene to acetylene on Ni(111).^{55,56} Hydrogen atoms are known to adsorb in 3-fold sites on Ni(110).⁵⁷ Hydrogen atom detachment would likely be the most facile for the cis- $C_2H_2D_2$ isomer because the hydrogen atoms could occupy the sites on one side of the row and the C_2D_2 product could reside in the trough on the other side of the Ni row. Of the three $C_2H_2D_2$ isomers, the cis- $C_2H_2D_2$ is observed to be the easiest to dehydrogenate with the STM. Similarly, the reduction in the availability of sites for the C_2D_2 product could be responsible for the relative difficulty of trans- $C_2H_2D_2$ dehydrogenation. Therefore, the observed threshold voltage suggests that the loss of two hydrogen atoms is the more likely mechanism compared to H_2 elimination. However, it cannot be determined whether the two hydrogen atoms are eliminated concomitantly or sequentially.

The dehydrogenation of acetylene produces two carbon atoms that are separated by 5.0 Å in Figure 8e. This distance between the carbon atoms is significantly larger than the C–C distance calculated for acetylene²⁴ or ethylene³⁰ on Ni(110), 1.3 and 1.4 Å, respectively. Thus, the data suggests that the STM-

induced dehydrogenation of acetylene is accompanied by the dissociation of the carbon–carbon bond.

Conclusions

The STM can be used to characterize and induce chemistry of single adsorbed molecules. Tunneling electrons were used to induce and monitor the hopping motions of ethylene adsorbed on Ni(110) at 13 K. The different isotopes exhibited characteristic hopping rates which can be used for chemical identification. A similar method was used to induce the dehydrogenation of individual ethylene molecules to acetylene, which was further reduced to carbon atoms. The threshold voltage for the dehydrogenation reactions was found to vary for the different isotopes. Theoretical modeling is needed to gain deeper insights into the mechanisms of the hopping motion and of the dehydrogenation. It is demonstrated, however, that the STM has the chemical sensitivity through vibrational spectroscopy to identify the different adsorbed molecules and reaction products at the single molecule level.

Observing and inducing the chemistry of single molecules provides insights into the dynamics that are unobtainable through studying the chemistry of an ensemble of molecules. It is possible to have precise knowledge of the local environment of each reactant and product molecule. The motions of single ethylene molecules before dissociation can be studied, yielding information through isotope studies, about the potential energy surface. Two distinct ethylene dehydrogenation products have been observed, S- and L-acetylene. Single molecule spectroscopy enables us to identify each individual product molecule.

Single molecule vibrational spectroscopy performed with the STM should prove to be useful in identifying the products of more complex reactions involving bond breaking and formation. In addition, STM-IETS allows the probing of the effects of coadsorbed species and of the surface on the intramolecular bonds. Results from these studies will further our understanding of the interactions between adsorbed molecules and enable a fuller understanding of the local environment involved in reactions.

Acknowledgment. Support of this work by the Cornell Center for Materials Research (CCMR) through the National Science Foundation Grant No. DMR-9632275 and by the National Science Foundation Grant No. DMR-9417866 is gratefully acknowledged. In addition, we thank John T. Yates, Jr., for pointing out the role of the excited state in the isotope selectivity of ethylene dehydrogenation and William A. Goddard, III, for illuminating discussions on hydrocarbon chemistry.

JA991218S

(55) Bao, S.; Hofmann, P.; Schindler, K. M.; Fritzsche, V.; Bradshaw, A. M.; Woodruff, D. P.; Casado, C.; Asensio, M. C. *J. Phys.: Condens. Matter* **1994**, *6*, L93–L98.

(56) Bao, S.; Hofmann, P.; Schindler, K. M.; Fritzsche, V.; Bradshaw, A. M.; Woodruff, D. P.; Casado, C.; Asensio, M. C. *Surf. Sci.* **1995**, *323*, 19–29.

(57) Voigtländer, B.; Lehwald, S.; Ibach, H. *Surf. Sci.* **1989**, *208*, 113–135.